

Imidazolium Ionic Liquids, Imidazolylidene Heterocyclic Carbenes, and Zeolitic Imidazolate Frameworks for CO₂ Capture and Photochemical Reduction

Sibo Wang and Xinchun Wang*

carbenes · carbon dioxide fixation · ionic liquids ·
metal–organic frameworks · photocatalysis

Imidazolium ionic liquids (ILs), imidazolylidene N-heterocyclic carbenes (NHCs), and zeolitic imidazolate frameworks (ZIFs) are imidazolate motifs which have been extensively investigated for CO₂ adsorption and conversion applications. Summarized in this minireview is the recent progress in the capture, activation, and photochemical reduction of CO₂ with these three imidazolate building blocks, from homogeneous molecular entities (ILs and NHCs) to heterogeneous crystalline scaffolds (ZIFs). The developments and existing shortcomings of the imidazolate motifs for their use in CO₂ utilizations is assessed, with more of focus on CO₂ photoredox catalysis. The opportunities and challenges of imidazolate scaffolds for future advancement of CO₂ photochemical conversion for artificial photosynthesis are discussed.

1. Introduction

In nature, green plants efficiently capture sunlight to convert CO₂ and water into various hydrocarbons and O₂, by photosynthesis, in a series of cascade reactions catalyzed by specific metalloenzymes.^[1] Fossil fuels were derived from photosynthetic activity over millions of years and currently supply us with most of the energy required to support everyday life. However, with the advancement of human society, especially the Industrial Revolution, huge amounts of fossil fuels have been expended, and their accompanying combustion has resulted in an increase in the concentration of atmospheric CO₂, which is intimately related to climate change.

Recently, much concern has been focused on worldwide energy shortages and environmental problems.^[2] Exploiting renewable alternatives to fossil fuels and decreasing CO₂

emissions are important challenges faced by modern society. Sunlight-driven photocatalytic CO₂ reduction toward artificial photosynthesis for the generation of energetic molecules (e.g., CO, HCOOH, CH₃OH, and

CH₄) using solar technology has been accepted as one of the most promising solutions, and would simultaneously solve both of the aforementioned problems in a carbon-neutral fashion by decreasing atmospheric CO₂ levels and providing valuable chemicals/fuels for energy.^[3]

However, photoredox CO₂ reduction catalysis is a rather challenging task because of the extremely stable characteristics of linear CO₂ molecules.^[4] The efficient transformation of CO₂ requires a catalyst which enables the capture, activation, and subsequent reduction of CO₂ molecules by proton-coupled multielectron transport to prevent the formation of thermodynamically unfavorable high-energy intermediates.^[5] Principally, the search for photocatalytic materials for CO₂ conversion encompasses conventional metal semiconductors^[6] and metal-decorated zeolites,^[7] as well as noble-metal-containing complexes.^[8]

Recent developments in CO₂ utilization chemistry involving organocatalysts^[9] and metal–organic frameworks (MOFs),^[10] where imidazolate motifs can serve as multifunctional organic groups for the capture, activation, and photo-reduction of CO₂, have attracted much interest. However, the literature contains no timely review which emphasizes the area of imidazolate motifs for CO₂ management, particularly the photofixation of CO₂ with visible light under mild reaction

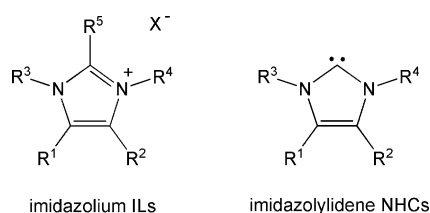
[*] S. Wang, Prof. X. Wang
State Key Laboratory of Photocatalysis on Energy and Environment
College of Chemistry, Fuzhou University
Fuzhou 350002 (China)
E-mail: xcwang@fzu.edu.cn
Homepage: <http://wanglab.fzu.edu.cn>

conditions, which is a very exciting and emerging research theme.

In this minireview, we summarize the latest progress with three imidazolate motifs [i.e., imidazolium ionic liquids (ILs), imidazolylidene N-heterocyclic carbenes (NHCs), and zeolitic imidazolate frameworks (ZIFs)] as building blocks for CO₂ utilization from homogeneous molecular entities to heterogeneous crystalline scaffolds. We believe a well-timed and comprehensive review on imidazolate scaffolds for CO₂ management is important and desirable to provide inspiring perspectives for future developments, especially on the photoconversion of CO₂ for artificial photosynthesis. Previous reviews, which have partially mentioned certain topics on CO₂ utilization involving imidazolate motifs, can supplement some of the detailed information which is beyond the scope of this article.^[9,10a,11]

2. Imidazolate Motifs of Imidazolium ILs, Imidazolylidene NHCs, and ZIFs

1) Imidazolium ILs,^[12] which are a class of homogeneous molecular building blocks with imidazolate motifs, are low-temperature molten salts formed by a weak combination of large imidazolate organic ions and charge-delocalized inorganic/organic anions (Scheme 1). Imidazolium ILs possess



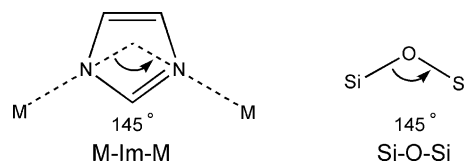
Scheme 1. General structure of imidazolium ILs and imidazolylidene NHCs.

distinct properties, including negligible volatility, high stability, high ionic conductivity, high polarity, and good solubility with many compounds. Therefore, these ILs have found applications in various fields, including separation, catalysis, materials synthesis, and photoelectric conversion.^[13]

2) Imidazolylidene NHCs represent another type of organic molecular building block with an imidazolate motif,

and these NHCs are typically derived from the corresponding imidazolium IL precursors by deprotonation at the C2-position (Scheme 1).^[14] Because of their versatile chemical functions, imidazolylidene NHCs have attracted extensive interest in the capture, activation, and fixation of CO₂ in recent years,^[9a] as well as for catalysis and other applications.^[15]

3) ZIFs,^[16] which are a subclass of MOFs, are porous crystalline materials which are fabricated from tetrahedral transition-metal ions (e.g., Zn or Co) and imidazolate (Im) ligands, and thus provides a family of heterogeneous building blocks with imidazolate motifs. In ZIFs, the bridging angle of M-Im-M is similar to the Si-O-Si angle of zeolites (Scheme 2),



Scheme 2. Representations of the M-Im-M angle of ZIFs and the Si-O-Si angle of zeolites.

thus creating ZIFs with a large number of zeolite-type tetrahedral topologies. ZIFs feature permanent porosity along with high thermal and chemical stabilities, and has resulted in ZIFs receiving much attention for use in CO₂ adsorption, separation, and conversion.^[17] In particular, the application of ZIFs for CO₂ photosplitting in solar to chemical energy conversion has recently emerged as an active area of research.^[10a,18]

3. Imidazolium ILs for the Capture, Activation, and Photoreduction of CO₂

3.1. Imidazolium ILs for CO₂ Capture

Numerous studies have confirmed that imidazolium ILs exhibit high capability for CO₂ capture.^[19] Brennecke and co-workers determined that CO₂ was extremely soluble in 1-butyl-3-methylimidazolium hexafluorophosphate ([BMIM][PF₆]), with a mole fraction reaching 0.6 at 8 MPa. However, the ILs did not appreciably dissolve in the CO₂-rich phase



Xinchun Wang is a professor at the State Key Laboratory of Photocatalysis on Energy and Environment, College of Chemistry, Fuzhou University. He obtained his B.S. from Fuzhou University and his Ph.D. from the Chinese University of Hong Kong. He was a postdoctoral fellow at Tokyo University, and an Alexander von Humboldt Fellow and group leader at the Max Planck Institute of Colloids and Interfaces. His interests are designing covalent carbon nitrides and MOFs for photocatalytic water splitting, CO₂ reduction, and organocatalysis.



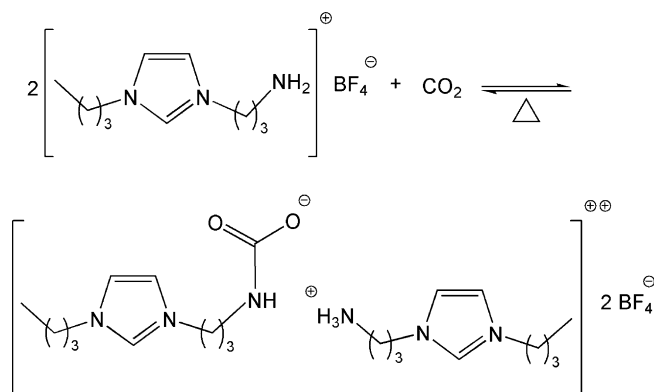
Sibao Wang received his B.S. degree in chemistry from Anqing Normal University (2010). He is now pursuing his Ph.D. in Prof. X. Wang's group at the State Key Laboratory of Photocatalysis on Energy and Environment, College of Chemistry, Fuzhou University. His research mainly focuses on the synthesis of MOFs and the study of MOFs for photocatalytic CO₂ reduction and water splitting.

even at 40 MPa.^[20] The absorption of CO₂ in [BMIM][PF₆] was reversible because the pure IL remained after the dissolved CO₂ was removed. These features indicate that the ILs can extract solutes from supercritical CO₂ without cross-contamination. By using systematic investigations in their next study,^[21] the group of Brennecke further demonstrated that CO₂ solubility in imidazolium-based ILs was dependent on both the substituents on the cation and the nature of the anion. ILs with anions bearing fluoroalkyl groups exhibited a greater capacity for CO₂ capture, while the ILs with longer alkyl chains on their imidazolium ring favored the absorption of CO₂.

To elucidate why imidazolium-based ILs exhibit such a high capacity for solubilizing CO₂, experimental and molecular modeling investigations were carried out by several groups.^[22] Cadena et al. conducted experimental investigations and molecular simulations to gain insights into the underlying mechanisms of CO₂ adsorption in alkyimidazolium-based ILs.^[22a] They observed that, in the interactions between the ILs and CO₂, the anion governs the primary contribution, whereas the cation plays a secondary role. In addition, the substitution of the acidic C2 hydrogen of the imidazolium cation with a methyl group decreased the experimental enthalpy of CO₂ absorption by about 1–3 kJ mol⁻¹, along with a minor perturbation in the organization of the anion and CO₂ around the cation. Furthermore, Berne and co-workers demonstrated that most of the space occupied by CO₂ in the imidazolium IL phase consists of extremely localized cavities which are for the most part formed by small angular rearrangements of the anions.^[22b] With these small angular rearrangements that do not significantly change radial distribution functions in the imidazolium ILs, CO₂ is able to fit above and below the imidazolium ring. These studies provided a comprehensive understanding of the ability of imidazolium-based ILs for CO₂ capture and offered a roadmap for the rational design and exploration of applications of imidazolium-based ILs in other fields (e.g., materials synthesis, catalysis, and biochemistry).

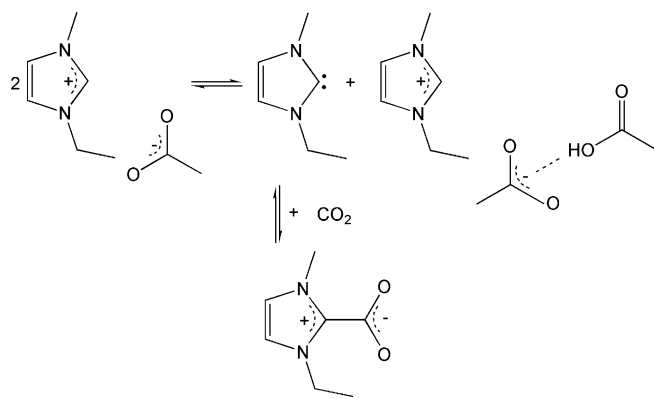
Davis and co-workers first reported an amine-functionalized task-specific IL (TSIL), having imidazolate motifs, for use in CO₂ capture.^[23] One mole of the IL could capture 0.5 moles of CO₂ in 3 hours under ambient pressure, thus affording a gravimetric capacity of about 7.4 % (Scheme 3). When the imidazolium IL was heated at 80–100 °C under vacuum for several hours, the captured CO₂ was extruded from the imidazolium IL. The recovered IL was repeatedly utilized for CO₂ capture for five cycles without a detected loss in efficiency. After the TSIL was treated with CO₂, a new absorption peak at 1666 cm⁻¹ in the FT-IR spectrum and a new resonance observed at δ = 158.11 ppm in the ¹³C NMR spectrum indicated the formation of a carbamate carbonyl carbon center, thereby revealing the chemisorption characteristics. However, the relatively high viscosity of the TSIL is unfavorable for CO₂ capture kinetics, which restricts its practical use in CO₂ scrubbing applications.

In 2011, the group of Rogers demonstrated the chemisorption of CO₂ by 1,3-dialkylimidazolium acetate ILs.^[24] When CO₂ was reacted with 1-ethyl-3-methylimidazolium acetate ([C2mim][OAc]) for 24 hours under atmospheric



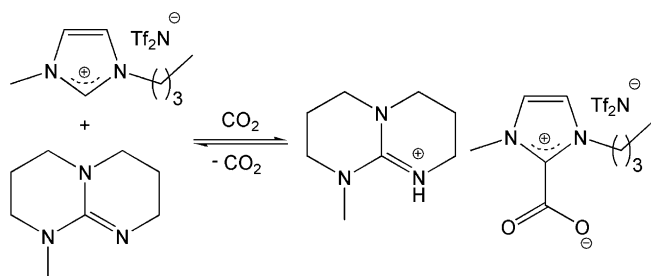
Scheme 3. Proposed reaction between imidazolium amine-functionalized TSIL and CO₂. Reprinted with permission from the American Chemical Society; see Ref. [23].

pressure and ambient temperature, the produced imidazolium carboxylate [i.e., 1-ethyl-3-methylimidazolium-2-carboxylate ([C2mim⁺-COO⁻])] was detected by NMR spectroscopy (Scheme 4). The clear liquid mixture solidified when the reaction was conducted for a longer time period (36 h) or under elevated pressure (20 bar). For the first time, the crystal structure of the formed solid-state products was determined by single-crystal X-ray diffraction analysis, and confirmed the formation of imidazolium carboxylate. The results of this study indicated that the ability of the anion to complex with any generated acid should be reconsidered as a factor for using these ILs. In addition, the ions of these ILs should not always be considered independently.



Scheme 4. Proposed reaction of CO₂ and [C2mim][OAc]. Reproduced with permission from the Wiley-VCH; see Ref. [24].

By virtue of the intrinsic acidity of the hydrogen at the C2-position in the imidazolium cation, Dai and co-workers achieved equimolar CO₂ absorption using imidazolium ILs integrated with organic superbases.^[25] The reaction of CO₂ with an imidazolium IL which contains an equimolar amount of superbase produced a liquid carboxylate salt, which demonstrated the equimolar capture of CO₂ with this hybrid system (Scheme 5). The combined imidazolium IL/superbase system achieved quick and reversible CO₂ capture with



Scheme 5. Equimolar CO₂ capture by an imidazolium IL and superbase system. Reproduced with permission from the Royal Society of Chemistry; see Ref. [25]. Ts = 4-toluenesulfonyl.

a stoichiometry of approximately 1:1 and exhibited high reusability. This study provided a promising strategy for CO₂ capture without the use of volatile alkanols, amines, or water. At almost the same time, Dai et al. reported reversible CO₂ capture by superbase-derived protic imidazolium ILs which exhibited an extremely high capacity (greater than a 1:1 ratio).^[26] Because the polarity and basicities of protic ILs can be readily switched, this study offered imidazolium ILs with potential applications in catalysis and separation.^[27]

3.2. Imidazolium ILs for CO₂ Activation

With the prerequisite of excellent capability for CO₂ capture, imidazolium ILs have the ability to activate and subsequently convert CO₂ into fuels or other useful chemicals.^[28] In 2003, the group of Deng reported imidazolium ILs/CsOH-catalyzed CO₂ activation for the synthesis of symmetric urea derivatives without the participation of stoichiometric quantities of a dehydrating agent.^[29] The yield of the targeted products was determined by the type of cations and anions in the ILs. When water was added to the reaction mixture, the imidazolium ILs were easily separated from the products, thus ensuring the reusability of the ILs. Control experiments revealed that, once the imidazolium ILs were removed, the production of urea derivatives was nearly zero, and suggests the necessity of imidazolium ILs for CO₂ activation and successive CO₂ utilization reactions. This study provided a facile, green, and reproducible method for the synthesis of urea derivatives from amines and CO₂ using imidazolium ILs.

Han and co-workers developed an imidazolium-IL-promoted CO₂ hydrogenation catalytic reaction to produce HCOOH using a ruthenium-immobilized heterogeneous catalyst [“Si”-(CH₂)₃NH(C₈H₅)-RuCl₃-PPh₃].^[30] With the presence of a tertiary amino group on the cation, the synthesized basic imidazolium IL [i.e., 1-(*N,N*-dimethylaminoethyl)-2,3-dimethylimidazolium trifluoromethanesulfonate ([mammim][TfO)] reacted with the generated HCOOH to form a salt, which led to facile separation for reuse. The catalytic system exhibited satisfactory activity and selectivity without the involvement of either organic solvents or generation of waste. An intriguing characteristic of this IL-supported CO₂ fixation system was the facile recovery of the catalyst, product, and imidazolium IL using a simple proce-

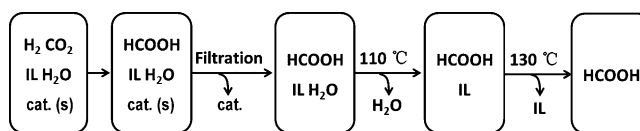


Figure 1. CO₂ hydrogenation reaction and recovery of the product, catalyst, and imidazolium IL. Reproduced with permission from the Wiley-VCH; see Ref. [30].

cedure (Figure 1), which is beneficial for the practical application of this chemical system.

In 2011, the group of Masel reported a significant discovery on CO₂ activation and reduction using an imidazolium IL [i.e., 1-ethyl-3-methylimidazolium tetrafluoroborate (EMIM-BF₄)].^[31] The one-electron reduction of CO₂ to the “CO₂^{•-}” intermediate requires high activation energy because of the rather negative equilibrium potential of the reaction.^[32] The formation of CO₂^{•-} in EMIM-BF₄ was most likely promoted by the manner of CO₂ complexation with the IL (Figure 2a). The CO₂ to CO reduction reaction occurred on a silver cathode with the imidazolium IL as a CO₂ activator.

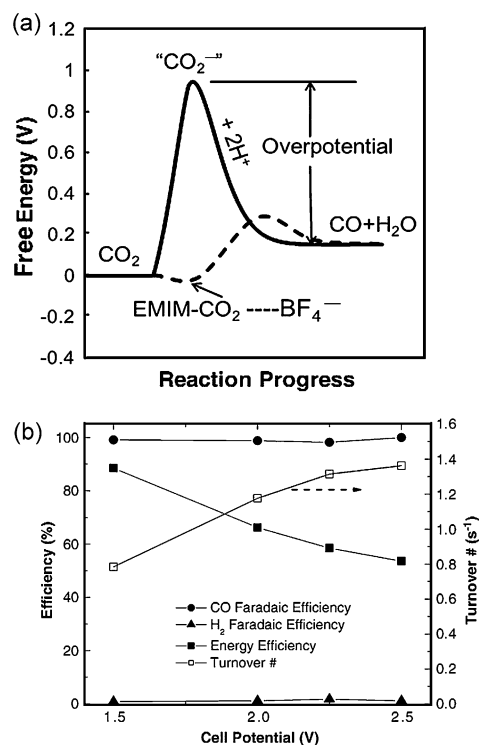


Figure 2. a) A schematic representation of how the free energy of the system changes during the reaction: CO₂ + 2H⁺ + 2e⁻ → CO + H₂O in water or acetonitrile (solid line) or EMIM-BF₄ (dashed line). b) Plot of the Faradaic efficiency of the process to form the desired CO and the undesired hydrogen, and the turnover rate as a function of applied cell potential. Reproduced with permission from the Nature Publishing Group; see Ref. [31].

In the EMIM-BF₄-accelerated CO₂ reduction system, CO was generated at an applied voltage of 1.5 V, which afforded an overpotential of only about 0.17 V for the reaction because of the equilibrium potential of the CO₂ to CO conversion

reaction being 1.33 V [Eq. (1)]. However, when the reaction was operated in an electrolyte without EMIM-BF₄, CO did not form until a potential of 2.1 V was applied, and indicates the crucial role of the imidazolium IL in CO₂ activation and subsequent conversion into CO.



The Ag-EMIM-BF₄-catalyzed CO₂ reduction system exhibited a Faradaic efficiency higher than 96% for CO generation and less than 3% for hydrogen evolution (Figure 2b). The catalytic turnovers (calculated according to the electrochemical surface area of the cathode catalysts) reached 26 000 when the reaction was performed at 2.5 V for 7 hours. Although the system has limited commercial potential (e.g., low catalytic rate, small surface area of the electrodes, and high cost of the electrodes and membrane), the results from this study demonstrated a breakthrough for the use of imidazolium ILs for CO₂ reduction electrocatalysis with respect to a low activation energy and high Faradaic efficiency. Significantly, this work revealed the stabilizing effect of imidazolate motifs on the CO₂^{•−} radical in CO₂ activation, which may be of particular interest in CO₂ fixation and artificial photosynthesis. However, one concern of halide-containing (e.g. [BF₄][−], [PF₆][−]) imidazolium-based ILs is that they are hydrolytically instable, thus releasing HF. This instability may impact the effects of imidazolium ILs for CO₂ adsorption and other utilization (e.g. CO₂ photoreduction as will be discussed later on).^[33]

3.3. Imidazolium ILs for CO₂ Photoreduction

On the basis of the ability of imidazolate motifs to stabilize the CO₂^{•−}, in 2013 Wang and co-workers achieved photocatalytic CO₂ reduction to CO promoted by imidazolium ILs under ambient conditions.^[34] The visible-light-driven CO₂ reduction reaction was conducted in a mixture consisting of an imidazolium IL (EMIM-BF₄) and water, along with [Ru(bpy)₃]Cl₂ (bpy = 2,2'-bipyridine), CoCl₂·6H₂O, and triethanolamine (TEOA) as a light sensitizer, an electron mediator, and an electron donor, respectively. Therefore, the developed CO₂ reduction protocol combined imidazolate IL chemistry with photoredox organocatalysis to achieve artificial photosynthesis.

Under typical reaction conditions, the CO₂ molecules were photocatalytically reduced to CO at a reaction rate of 15.5 μmol h^{−1} and with an H₂ evolution rate of 2.1 μmol h^{−1}. The indispensable role of the imidazolium IL for the CO₂ reduction reaction was demonstrated by the observation that the reaction was completely terminated when the IL was removed. In addition, when EMIM-BF₄ was replaced by HBF₄, no products were generated. These observations indicated the significant role of the imidazolate motif for the catalysis of CO₂ conversion, that is, the imidazolate motif not only facilitates CO₂ adsorption but also promotes CO₂ activation by reducing the potential for the formation of CO₂^{•−} and the overall barrier of the redox reaction.

Wang et al.^[34] performed the CO₂ to CO transformation reaction in various media to examine the universality of the imidazolium IL for supporting CO₂ conversion catalysis. The results indicated that the CO₂ reduction reaction was substantially improved in all of the studied solvents when EMIM-BF₄ was added (Figure 3), thus indicating the generality of the ILs to boost the CO₂ conversion reaction in diverse media.

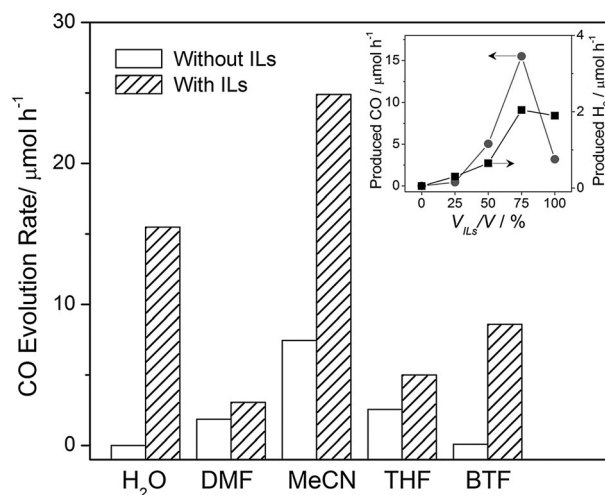


Figure 3. Promotional effect of ILs on CO₂ photofixation in various solvents. The inset shows the effect of the [EMIM][BF₄]/H₂O ratio on the photocatalytic reduction of CO₂. Reproduced with permission from the Nature Publishing Group; see Ref. [34]. BTF = benzenyltrifluoride, DMF = *N,N*-dimethylformamide, THF = tetrahydrofuran.

To gain additional insight into the effect of imidazolium ILs on CO₂ photofixation, various ILs (with different counterions or substitutes; Figure 4) were applied to the developed CO₂ reduction system. The efficiency of the CO₂ reduction catalyst was largely affected by the type of the counterions. The TfN₂[−] anion exhibited the greatest promotional effect for the CO₂ photoreduction reaction compared to the other studied anions (i.e., L-L[−], TfO[−], Ac[−], DCA[−], and BF₄[−]). The substituents on the 1-position of the imidazolium ring also greatly influenced the catalytic activity. When the alkyl chain was elongated from ethyl to octyl, the yield of CO/H₂ decreased. These results indicated that the counterions and organic functional groups of the imidazolium ILs strongly determine their ability to promote CO₂ photoreduction catalysis.

In the study by Wang et al.,^[34] the use of imidazolium ILs was delineated as a homogeneous organic molecular building block for the activation and photoredox transformation of CO₂. Therefore, IL chemistry was extended to artificial photosynthesis reactions, a promising, intriguing, and emerging research topic that we believe will attract considerable attention in the future for CO₂ fixation and advanced photosynthesis (e.g., the coupling of CO₂ reduction and overall water splitting).

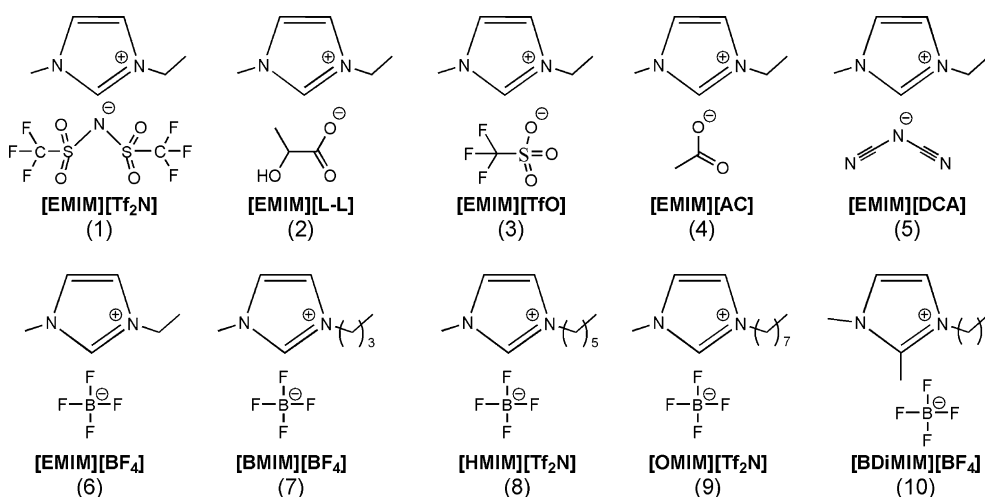
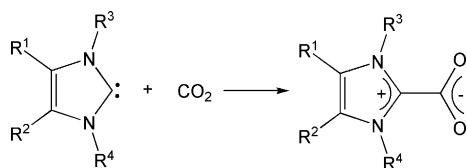


Figure 4. Chemical structures of the various imidazolium ILs studied in the photoreduction of CO₂ into CO in Ref. [33]. Reproduced with permission from the Nature Publishing Group; see Ref. [34].

4. Imidazolylidene NHCs for the Capture, Activation, and Photoconversion of CO₂

4.1. Imidazolylidene NHCs for CO₂ Capture

Because of the existence of a lone pair of electrons, imidazolylidene NHCs is known as a nucleophile which can capture CO₂ to form imidazolium carboxylate (referred to as the NHC–CO₂ adduct; Scheme 6).^[35] In the formed NHC–



Scheme 6. Imidazolylidene NHCs for the capture of CO₂ to form NHC–CO₂ adducts.

CO₂ scaffold, the bonds of CO₂ were bent with an angle of about 130°, which indicates that the very stable and linear CO₂ molecule was activated. For example, in 2004 Louie et al. reported the reversible carboxylation of free imidazolylidene NHCs with CO₂ to synthesize zwitterionic NHC–CO₂ adducts by simple deprotonation of imidazolium ILs with potassium *tert*-butoxide under a CO₂ atmosphere.^[36] The formed NHC–CO₂ adducts can be used as precursors to efficiently transfer NHCs for subsequent reaction by liberation of CO₂, thus circumventing the troublesome separation of water- and air-sensitive free NHCs.

Density-functional theory (DFT) studies have also been conducted by several groups to provide theoretical support for CO₂ capture and fixation using imidazolylidene NHCs.^[37] In 2011, Ajitha and Suresh assessed the influence of stereoelectronic factors on the CO₂ capture and fixation ability of NHCs using DFT modeling.^[38] They concluded that the use of an N-substituent, such as CH₂OH, CH₂NHCOMe,

or CH₂NHPh, would significantly improve the CO₂-fixing ability of NHCs. Lo and Ganguly performed DFT simulations of NHC/superbase systems for CO₂ adsorption with alcohols, and predicted the steric and electronic effects of the carbenes which play a key role in determining the mode of CO₂ capture.^[39] Recently, Ashfeld and co-workers executed DFT calculations and experimental measurements to investigate the binding of CO₂ to an imidazolylidene NHC, and thus demonstrated rapid and stoichiometric solid-phase covalent CO₂ capture at a relatively low pressure.^[40]

For translating the function of NHCs for CO₂ capture from homogeneous to heterogeneous modes, polymerization strategies have been developed for CO₂ capture using polymers possessing NHC ligands. In 2009, a highly efficient imidazolylidene NHC-functionalized polymer for the reversible capture/release of CO₂ was described by the group of Lu (Figure 5).^[41] The zwitterionic polymer NHC–CO₂ adduct was formed after rapid reaction between CO₂ and the immobilized NHC at 20–100 °C. In addition, the fixed CO₂ was completely released under an N₂ flow at 140 °C. These results demonstrated the potential of NHC scaffolds for CO₂ capture in a heterogeneous fashion, which has greater potential for practical applications considering their ease of separation and recovery.

4.2. Imidazolylidene NHCs for CO₂ Activation and Conversion

Imidazolylidene NHCs have been widely studied as homogeneous organocatalysts for activating and converting CO₂ into value-added products. In 2009, Zhang and Gu reported NHC-catalyzed CO₂ splitting reactions to produce CO using aromatic aldehydes as oxygen acceptors (Figure 6).^[42] The best result was achieved when the reaction was carried out in dimethylsulfoxide (DMSO) containing a potassium carbonate additive, where the yield was about 95%. Zhang and Gu proposed a catalytic mechanism, in which they hypothesized that the imidazolylidene NHC directly activated

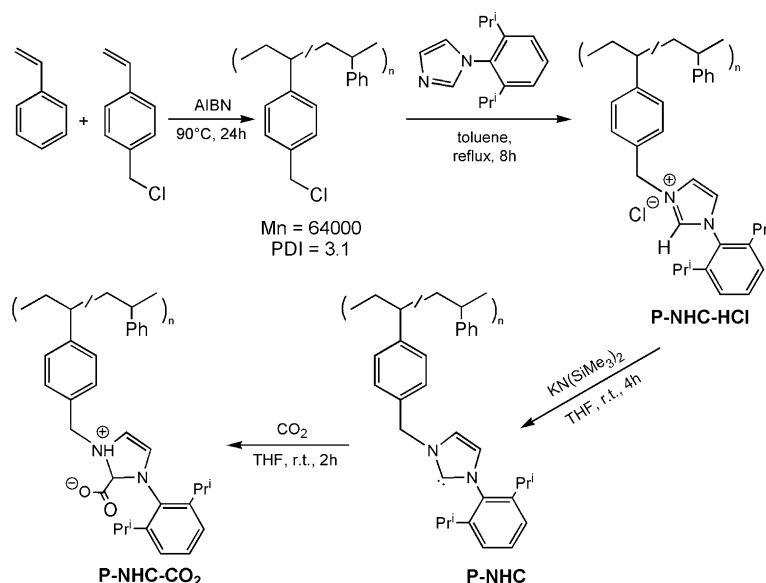


Figure 5. Synthesis of copolymer-bearing imidazolydene NHC and its use for CO₂ capture. Reprinted with permission from the American Chemical Society; see Ref. [41]. AIBN = 2,2'-azobis(isobutyronitrile).

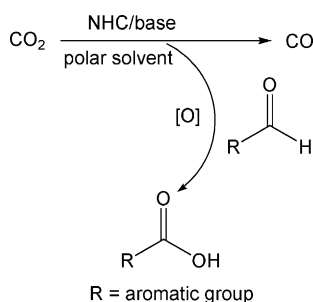


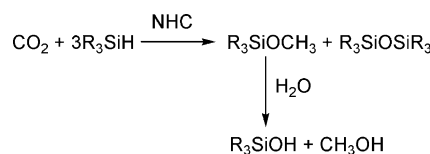
Figure 6. CO₂ splitting reaction with an aldehyde catalyzed by imidazolydene NHC. Reprinted with permission from the American Chemical Society; see Ref. [42].

CO₂ to form imidazolium carboxylate.^[42] However, the carbene chemistry for CO₂ adsorption/conversion is very moisture sensitive.

Metal/NHC scaffolds are extensively investigated types of building blocks consisting of imidazolate motifs for CO₂ activation and conversion reactions. Among these reactions, copper/NHCs have attracted much attention.^[43] For example, Sadighi and co-workers reported the deoxygenative reduction of CO₂ to CO catalyzed by NHC-ligated copper boryl complexes under mild reaction conditions with considerable turnover numbers and frequencies.^[44] The group of Hou demonstrated that copper complexes bearing imidazolydene NHC motifs can act as efficient catalysts to synthesize diverse functionalized carboxylic acid derivatives by a carboxylation reaction of organoboronic esters with CO₂.^[45] In this reaction, the copper/NHC alkoxide complex was confirmed to be the active species. This complex was isolated and fully characterized, and the results provided important insights into the reaction mechanism. However, the use of a stoichiometric and expensive organometallic additive is a substantial drawback for the CO₂ transformation reaction.^[43c,45]

In 2011, Zhang and Yu presented the copper/NHC-catalyzed carboxylation reaction of terminal alkynes and CO₂ without an organometallic agent.^[46] They examined various copper/NHC catalysts using their established reaction protocol, and a series of propiolic acids were efficiently prepared under mild reaction conditions. A reaction mechanism was proposed (Figure 7) in which the copper center activated the terminal alkyne with a base to generate a copper acetylide species and the free NHC activated CO₂ to form the NHC-CO₂ adduct. Additionally, the use of other metal/NHC scaffolds (metal = Zn, Ni, Au, Pd) in CO₂ activation and fixation reactions has been reported.^[47] All of these studies demonstrated the significance of the imidazolate motifs in the NHC building blocks for CO₂ activation and subsequent transformations.

In addition to metal/NHC complexes, the metal-free silicon and boron NHCs containing imidazolate entities have been explored to directly catalyze CO₂ conversion reactions. Ying and co-workers reported the first metal-free reduction of CO₂ to CH₃OH catalyzed by NHCs, with silanes as the reductants and hydride donors (Scheme 7).^[48] ¹³C-labeled isotopic experiments confirmed that CO₂ was catalytically converted into methoxide products by hydrosilane. Under ambient conditions, the catalytic CO₂ conversion reaction rapidly proceeded, with a hydrogen-transfer yield as high as 90% to produce CH₃OH after a 24 hour reaction. This result



Scheme 7. Overall stoichiometric conversion reaction of CO₂ into CH₃OH, catalyzed by imidazolydene NHC. Reproduced with permission from the Wiley-VCH; see Ref. [48].

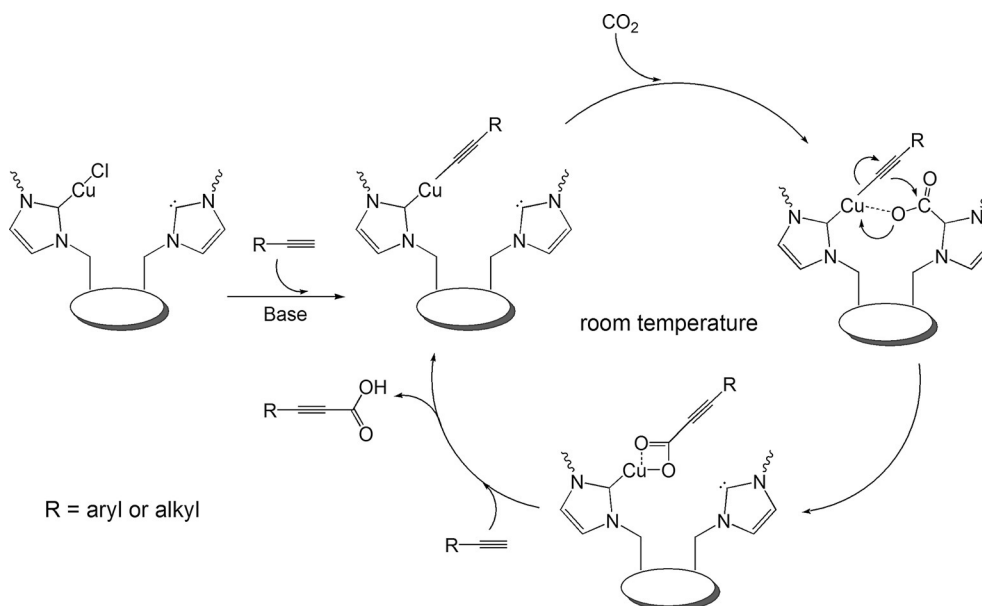
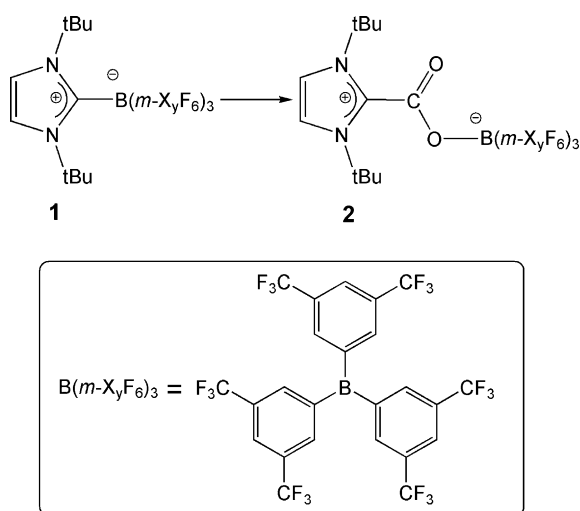


Figure 7. Copper-carbene cocatalyzed carboxylation mechanism for terminal alkynes and CO₂. Reprinted with permission from Ref. [46].

indicated the remarkable superior efficiency of NHCs compared to the efficiency of the reaction catalyzed by transition-metal catalysts. A possible reaction mechanism was also proposed according to the spectrometrically and spectroscopically detected intermediates. This study provided an intriguing strategy for CO₂ activation and conversion. However, the employment of a hydride donor is disadvantageous.

In 2012, Kolychev et al. introduced an NHC/boron adduct [also referred to as a frustrated Lewis pair (FLP)] for CO₂ fixation (Scheme 8).^[49] After the imidazolyliene NHC/borane salt **1** was exposed to CO₂ in benzene for 24 hours at room temperature, a high yield (86%) of the compound **2** was obtained in high purity. This research not only presented an example of NHC/boron scaffolds bearing an imidazolate motif as a nonmetal catalyst for CO₂ reduction under mild reaction conditions, but also indicated the role of the FLP



Scheme 8. Reaction of imidazolyliene NHC/borane adduct with CO₂. Reproduced with permission from Wiley-VCH; see Ref. [49].

as an imidazolate building block for CO₂ activation and fixation.

For the reaction mechanism of metal-free NHC in CO₂ activation and fixation, the group of Wang conducted DFT calculations to study the catalytic role of NHC in the CO₂ to CH₃OH conversion reaction.^[50] The predicted catalytic mechanism successfully supported their experimentally detected intermediates. However, CH₂O was predicted to be an unavoidable intermediate, which has not been experimentally verified.

Recently, Zhang and co-workers investigated the silane NHC-catalyzed reduction of CO₂ using a combination of experimental studies and DFT calculations.^[51] The reaction mechanism predicted by the group of Wang differed somewhat from the experimental and calculated findings of Zhang et al. because CH₂O was unlikely to be an intermediate in the reaction. The overall reaction pathway in the CO₂ reduction catalysis by NHCs with silanes consisted of a three-step cascade reaction. The imidazolyliene NHCs catalyzed all three exothermic processes, where the first step of hydrosilylation required the highest activation energy and was the rate-limiting step. This study provided additional insight into the metal-free NHC-catalyzed CO₂ activation and conversion reactions and should be of great importance for CO₂ fixation mediated by similar NHC scaffolds in the future.

Besides, NHC-catalyzed CO₂ cycloaddition reactions for the generation of cyclic carbonates have also garnered much attention with regard to CO₂ activation and fixation by imidazolate motifs. Ikariya and co-workers described the efficient carboxylative cyclization of terminal propargyl alcohols and epoxides with CO₂, catalyzed by NHCs bearing imidazolate entities (Figure 8).^[52] High yields of the corresponding cyclic carboxylates were obtained under relatively benign conditions. The mechanism for the cycloaddition catalytic reaction emphasized the capture and activation of CO₂ by the imidazolyliene NHC to form NHC-CO₂ adducts,

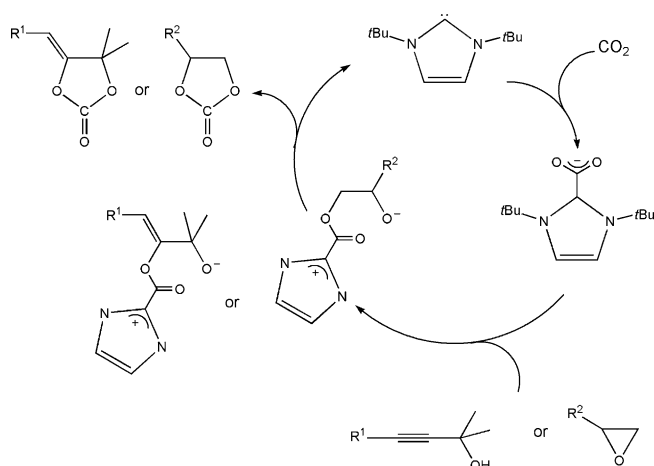


Figure 8. Reaction mechanism of the carboxylation reaction catalyzed by an imidazolylidene NHC- CO_2 adduct. Reproduced with permission from Wiley-VCH; see Ref. [52].

followed by the nucleophilic addition of imidazolium-2-carboxylate to either the C–C bond or the strained epoxide ring to the alkoxide intermediates. In the catalytic cycle, the bond between the CO_2 fragment and imidazolylidene NHC was determined to be a plausible rate-determining step. This study demonstrated imidazolylidene NHCs as efficient organocatalysts in CO_2 activation and fixation for the direct and solvent-free synthesis of carbonates.

4.3. Imidazolylidene NHC Motifs for CO_2 Photoconversion

Imidazolylidene NHCs have been extensively investigated for CO_2 capture, activation, and fixation. However, the operation of NHCs bearing imidazolate motifs for photocatalytic CO_2 reduction remains in its infancy. In 2013, Chang and co-workers reported visible-light photoredox catalysis for the deoxygenative reduction of CO_2 to CO using nickel/NHC/isoquinoline complexes, $[\text{Ni}(\text{Prbimiq1})]^{2+}$ [where Prbimiq1 = bis(3-(imidazolyl)isoquinoliny)propane], bearing imidazolate scaffolds (Figure 9).^[53] The authors first examined the electrocatalytic performance of the CO_2 to CO reduction reaction by the $[\text{Ni}(\text{Prbimiq1})]^{2+}$ complex and determined that the complex was an efficient electrocatalyst for CO_2

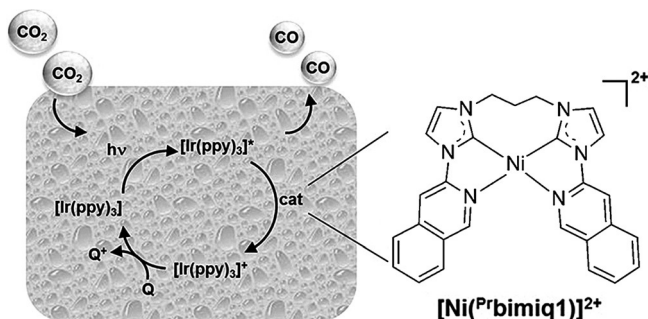


Figure 9. Photocatalytic CO_2 reduction to CO catalyzed by nickel NHC-isoquinoline complexes. Reprinted with permission from the American Chemical Society; see Ref. [53].

conversion, with a lowest cathodic onset potential of -1.2 V [versus the saturated calomel electrode (SCE)]. The photocatalytic CO_2 reduction system was constructed using $[\text{Ni}(\text{Prbimiq1})]^{2+}$ as a catalyst coupled to $[\text{Ir}(\text{ppy})_3]$ (ppy = 2-phenylpyridine) and triethylamine (TEA), which serve as a visible-light photosensitizer and electron donor, respectively.

The CO_2 photoreduction system exhibited high catalytic efficiency and afforded turnover numbers and turnover frequencies of 98000 and 3.9 s^{-1} , respectively (determined by CO production and the nickel NHC-isoquinoline complex). A high CO_2 reduction selectivity over protons was assumed because no detectable H_2 was formed. In comparison to irradiated semiconductor powders, this molecular photocatalytic system exhibited a twofold reinforced solar-to-fuel efficiency of 0.01 %. By using a series of control experiments, the authors claimed that the degradation of the photosensitizer was a limiting factor for extended CO_2 conversion but not deactivation of the $[\text{Ni}(\text{Prbimiq1})]^{2+}$ catalyst. They further proposed that its use in long-term CO_2 photofixation applications was possible. Despite the involvement of a noble-metal photosensitizer and sacrificial agent, this study integrated imidazolylidene NHC chemistry with photoredox engineering to convert CO_2 into a valuable product using a solar resource, thus revealing the ability of imidazolylidene NHC scaffolds to function as molecular building blocks bearing imidazolate motifs for application in solar-to-fuel transformation reactions for artificial photosynthesis. Very recently, Falvey and co-workers reported the photochemical reduction of CO_2 by 1,3-dimethylimidazolylidene through photolysis of an excited-state donor $[\text{N},\text{N},\text{N}',\text{N}'\text{-tetramethylbenzidine (TMB)}]$.^[54] Although the CO_2 conversion process in this study is not catalytic, it however further demonstrated the vitality of imidazolylidene NHCs as imidazolate motifs to promote CO_2 photoreduction.

5. ZIFs for the Capture, Conversion, and Photo-splitting of CO_2

5.1. ZIFs for CO_2 Adsorption

The group of Yaghi synthesized a series of ZIFs and examined their CO_2 adsorption properties.^[17a,b,55] As listed in Table 1, all of the studied ZIFs displayed efficient CO_2 adsorption capabilities, and some of the ZIFs exhibited CO_2 adsorption capabilities superior to that of BPL carbon. The CO_2 uptake isotherms of some ZIFs (i.e., ZIF-68, ZIF-69, ZIF-70) exhibited sharp adsorption at low pressures, thus reflecting their high affinity toward CO_2 . Importantly, the CO_2 adsorption-desorption behavior of certain ZIFs was completely reversible, thus indicating the possibility of using the ZIFs as excellent materials for CO_2 purification and landfill sequestration. In 2010, Yaghi and co-workers carried out a combination of experimental and computational research on CO_2 capture in five isoreticular ZIFs and investigated the effect of different functional groups on CO_2 uptake.^[56] The molecular modeling calculations revealed that functionalizing the imidazolate ligands with functional groups

Table 1: Surface area and CO₂ uptake for some ZIFs.^[55b]

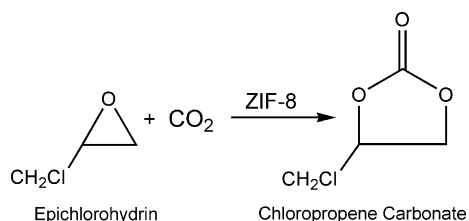
Material	BET [m ² g ⁻¹]	CO ₂ [cm ³ g ⁻¹]	CO ₂ [cm ³ cm ⁻³]
ZIF-68	1090	37.6	39.9
ZIF-69	950	40.6	49.2
ZIF-70	1730	55.0	45.4
ZIF-78	620	51.5	60.2
ZIF-79	910	33.5	36.1
ZIF-81	760	38.2	49.3
ZIF-82	1300	52.7	49.3
ZIF-95	1050	19.7	19.2
ZIF-100	595	32.6 ^[a]	28.2 ^[a]
BPL C ^[b]	1150	46.8	22.5

[a] Measured at 273 K. [b] BPL carbon was used for comparison.

that exhibit different polarizabilities and symmetries significantly influenced the CO₂ adsorption abilities of the ZIFs, and implied the important status of imidazolate motifs for CO₂ capture in metal–organic scaffolds. Recently, Zhang et al. reported the fabrication of a hybrid ZIF (ZIF-9-67) membrane on an α -Al₂O₃ support for efficient CO₂ adsorption.^[57] The membrane exhibited high gas permeance and good selectivity. This study revealed the CO₂-capture and separation capabilities of ZIFs stemming from the combined advantages of the ZIFs and membrane engineering.^[58] Compared with the commercially available materials (e.g. activated carbon, zeolites, etc.), the relatively complicated synthesis protocol of ZIFs may disfavor their general use for CO₂ adsorption in practical scale.

5.2. ZIFs for CO₂ Activation

In 2011, Carreon and co-workers reported the ZIF-8-catalyzed cycloaddition reaction of CO₂ with epichlorohydrin to produce chloropropene carbonate in the absence of cocatalysts and solvents (Scheme 9).^[59] The ZIF-8 catalyst



Scheme 9. Reaction of epichlorohydrin with CO₂ to produce chloropropene carbonate. Reprinted with permission from the American Chemical Society; see Ref. [59].

attained high epoxide conversion and moderate selectivity for chloropropene carbonate at a relatively low reaction temperature of 70 °C. Moreover, after functionalization with ethylenediamine, the modified ZIF-8 catalyst exhibited overall epichlorohydrin conversion and considerably improved cyclic carbonate selectivity. The promotion of the catalytic performance in functionalized ZIF-8 was ascribed to the high CO₂ affinity of the amino group, and was confirmed by the CO₂

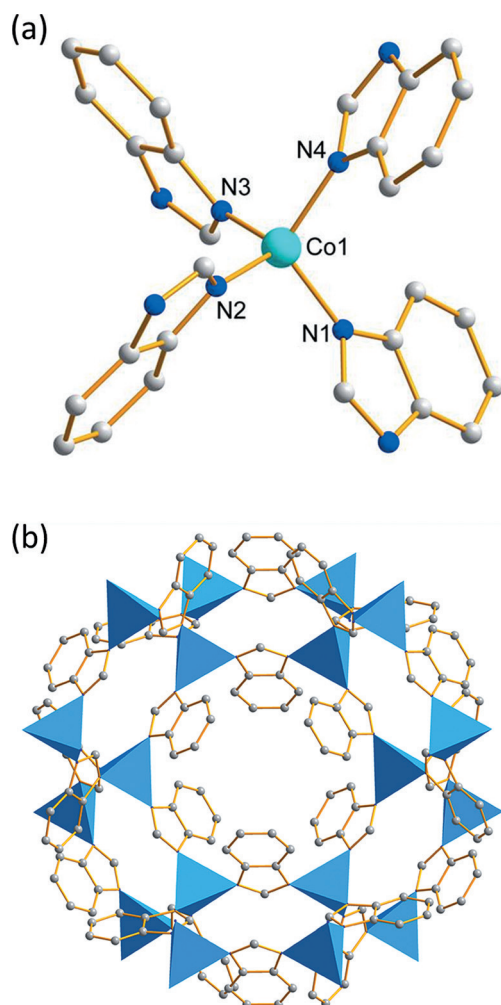
adsorption isotherms. The difficulty with the ZIF-8-mediated CO₂ conversion system was the loss of the high catalytic activity and the instability of ZIF-8 under the pressurized reaction conditions.

Very recently, Jose et al. introduced another efficient, cocatalyst and solvent-free CO₂ cycloaddition reaction for the synthesis of cyclic carbonates from allyl glycidyl ether by ZIF-90 functionalized with a quaternary ammonium group.^[60] Again, deactivation and instability of ZIF were encountered in the developed system. Although limitations exist in the ZIF-catalyzed CO₂ transformation systems, these studies indicated the vitality of ZIFs as heterogeneous building blocks with imidazolate motifs for CO₂ activation and conversion. We believe ZIF-catalyzed photocatalytic CO₂ reduction catalysis is promising in view of the advantages of the solar resource and the benignness of the reaction conditions.

5.3. ZIFs for CO₂ Photosplitting

In 2014, Wang and co-workers demonstrated CO₂ photosplitting catalysis using a cobalt-based ZIF (Co-ZIF-9;^[17c,61] Scheme 10) with a visible-light photosensitizer [Ru(bpy)₃]Cl₂ under mild reaction conditions.^[18] The photocatalytic CO₂ conversion reaction was conducted in a MeCN/H₂O solution with TEOA as a sacrificial agent. After photocatalysis for 30 minutes, the main detected CO₂ reduction product was CO, with a generation rate of 1.4 $\mu\text{mol min}^{-1}$, coupled with H₂ evolution rate of about 1.0 $\mu\text{mol min}^{-1}$. A control experiment determined that, in the absence of Co-ZIF-9, the CO₂ to CO transformation reaction was significantly restrained, thus indicating the promotional effect of Co-ZIF-9 for the reaction. The control experiment pointed out that the catalytic performance of the precursors (Co²⁺ and benzimidazole) was much smaller than that of the ZIF even in a homogenous system. Furthermore, when the metal–organic architecture of Co-ZIF-9 was destroyed (e.g., by calcination), its catalytic activity almost vanished completely. All of these observations highlighted the critical role of the metal–organic scaffolds of Co-ZIF-9 to synergistically enhance carrier transfer and CO₂ concentration for the CO₂ photoreduction reaction. Notably, the stability of the Co-ZIF-9 catalyst was confirmed by several studies (e.g., ICP, XRD, FTIR, and XPS).

Wang et al. further synthesized a series of MOFs and evaluated their CO₂ photoreduction activities in the established protocol (Table 2), and the results revealed the uniqueness of Co-ZIF-9 toward the CO₂ conversion reaction.^[18] When Co-MOF-74 (ligand: 2,5-dihydroxyterephthalic acid) was used instead of Co-ZIF-9, the yield of the products markedly decreased, and thereby indicated the significance of imidazolate motifs in the CO₂ photofixation reaction. When Mn-MOF-74 (ligand: 2,5-dihydroxyterephthalic acid) was employed as a catalyst to replace Co-ZIF-9, no promotion in CO evolution was achieved compared to that of the catalyst-free system. Therefore, the electron-mediating function of the cobalt species was essential for effectively running the reaction. As expected, other MOFs (entries 4 and 5) were



Scheme 10. Chemical structure of Co-ZIF-9: a) Ball-and-stick representation of the second building unit showing the coordination environment around cobalt. b) Packing diagram of Co-ZIF-9. Reproduced with permission from Wiley-VCH; see Ref. [18].

Table 2: Comparison of the cocatalytic functions of Co-ZIF-9 with those of other MOFs.^[a]

Entry	MOFs	CO [μmol]	H ₂ [μmol]	TON
1	Co-ZIF-9	41.8	29.9	89.6
2	Co-MOF-74	11.7	7.3	23.8
3	Mn-MOF-74	1.5	2.9	5.5
4	Zn-ZIF-8	2.1	2.4	5.6
5	Zr-Uio-66-NH ₂	1.2	2.2	4.3

[a] Detailed reaction conditions are provided in Ref. [18].

unable to effectively catalyze the reaction. On the basis of these control experiments, the origin of the high catalytic performance of Co-ZIF-9 for the CO₂ photosplitting reaction involved the synergetic effect of the cobalt species and the benzimidazolate entities for supporting CO₂ capture/activation and charge transfer, but spatially linked within the porous metal-organic frameworks.

This study demonstrated the first application of ZIFs as an efficient and stable catalyst for photocatalytic CO₂ conversion

to CO under mild reaction conditions. However, the long-term and large-scale application of the CO₂ reduction system is limited by the use of an expensive and unstable ruthenium/dye photosensitizer. Consequently, Wang and co-workers further explored semiconductors, including g-C₃N₄^[62] and CdS,^[63] as light transducers to function in cooperation with Co-ZIF-9 for photocatalytic CO₂ reduction and developed a ZIF and semiconductor-based hybrid heterogeneous protocol for effective CO₂ photofixation under ambient conditions. The systems exhibited greatly enhanced stability and higher activity than that of the ruthenium/dye photosensitizer. These studies revealed the role of ZIFs as heterogeneous crystalline building blocks with imidazolate motifs for artificial photosynthesis to convert CO₂ into energetic molecules.

6. Outlook

It is the capability of imidazolate motifs as multifunctional organic groups to form imidazolium ILs, imidazolylidene NHCs, and ZIFs that make them very promising for CO₂ capture, activation, and conversion, ranging from homogeneous molecular entities to heterogeneous metal-organic frameworks. All the three building blocks of imidazolate motifs have shown prodigious opportunities when cooperating with photosensitizers to establish catalytic cascades for the capture, activation, and photocatalytic conversion of CO₂. In comparison to their wide use in CO₂ capture, the application of imidazolate entities for CO₂ conversion, particularly CO₂ photoreduction with visible light, has received much less attention. Therefore, imidazolate motifs hold great potential for artificial photosynthesis using solar technology to generate renewable energy from CO₂ because of their distinct chemical functions for the absorption and activation of CO₂. The main challenges encountered with imidazolate scaffolds for photoredox CO₂ fixation catalysis are a) the exploration of more imidazolate motif candidates for CO₂ photofixation by solar energy, b) the construction of other photochemical CO₂ reduction systems based on imidazolate motifs to extend the distribution of reduction products, c) the discovery of economical and stable visible-light harvesters to replace the noble-metal-containing and typically unstable photosensitizers involved in the established photocatalytic systems, and d) elimination of the sacrificial electron donors in photocatalytic CO₂ transformations by imidazolate scaffolds. We anticipate that the coupling of photocatalytic CO₂ reduction with overall water splitting or organic oxidative synthesis may provide a promising method to tackle the existing challenges of imidazolate-motif-catalyzed photochemical CO₂ reduction for artificial photosynthesis, and is envisaged to motivate intensive investigations on other functional organic groups with nitrogen-rich molecules such as triazine-, heptazine-, porphyrin-, and adenine-based structures for CO₂ utilizations.^[64] In addition, the development of membranes/thin-films bearing imidazolate entities may become more attractive for functional nanodevices to enable the capture and photochemical/photoelectrochemical conversion of CO₂ into valuable chemicals in the future.

Acknowledgement

This work is supported by the National Basic Research Program of China (2013CB632405), the National Natural Science Foundation of China (21425309 and 21173043), the State Key Laboratory of NBC Protection for Civilian (SKLNBC2013-04K), and the Specialized Research Fund for the Doctoral Program of Higher Education (20133514110003).

How to cite: *Angew. Chem. Int. Ed.* **2016**, *55*, 2308–2320
Angew. Chem. **2016**, *128*, 2352–2364

- [1] J. Barber, *Chem. Soc. Rev.* **2009**, *38*, 185–196.
- [2] a) N. Armadori, V. Balzani, *Angew. Chem. Int. Ed.* **2007**, *46*, 52–66; *Angew. Chem.* **2007**, *119*, 52–67; b) M. Mikkelsen, M. Jorgensen, F. C. Krebs, *Energy Environ. Sci.* **2010**, *3*, 43–81.
- [3] a) A. J. Morris, G. J. Meyer, E. Fujita, *Acc. Chem. Res.* **2009**, *42*, 1983–1994; b) C. D. Windle, R. N. Perutz, *Coord. Chem. Rev.* **2012**, *256*, 2562–2570; c) F. Sastre, A. Corma, H. García, *Angew. Chem. Int. Ed.* **2013**, *52*, 12983–12987; *Angew. Chem.* **2013**, *125*, 13221–13225; d) J. Mao, K. Li, T. Peng, *Catal. Sci. Technol.* **2013**, *3*, 2481–2498; e) N. S. Lewis, D. G. Nocera, *Proc. Natl. Acad. Sci. USA* **2006**, *103*, 15729–15735.
- [4] T. Sakakura, J.-C. Choi, H. Yasuda, *Chem. Rev.* **2007**, *107*, 2365–2387.
- [5] J. Schneider, H. Jia, J. T. Muckerman, E. Fujita, *Chem. Soc. Rev.* **2012**, *41*, 2036–2051.
- [6] a) V. P. Indrakanti, J. D. Kubicki, H. H. Schobert, *Energy Environ. Sci.* **2009**, *2*, 745–758; b) K. R. Thampi, J. Kiwi, M. Gratzel, *Nature* **1987**, *327*, 506–508; c) T. Inoue, A. Fujishima, S. Konishi, K. Honda, *Nature* **1979**, *277*, 637–638; d) S. C. Yan, S. X. Ouyang, J. Gao, M. Yang, J. Y. Feng, X. X. Fan, L. J. Wan, Z. S. Li, J. H. Ye, Y. Zhou, Z. G. Zou, *Angew. Chem. Int. Ed.* **2010**, *49*, 6400–6404; *Angew. Chem.* **2010**, *122*, 6544–6548.
- [7] a) H. Yamashita, K. Ikeue, M. Anpo, *CO₂ Convers. Util.* **2002**, *22*, 330–343; b) M. Matsuoka, M. Anpo, *J. Photochem. Photobiol. C* **2003**, *3*, 225–252; c) W. Lin, H. Frei, *J. Am. Chem. Soc.* **2005**, *127*, 1610–1611.
- [8] a) J. M. Lehn, R. Ziessel, *Proc. Natl. Acad. Sci. USA* **1982**, *79*, 701–704; b) J. Ettinger, Y. Diskin-Posner, L. Weiner, R. Neumann, *J. Am. Chem. Soc.* **2011**, *133*, 188–190; c) Y. Tamaki, T. Morimoto, K. Koike, O. Ishitani, *Proc. Natl. Acad. Sci. USA* **2012**, *109*, 15673–15678; d) G. A. Andrade, A. J. Pistner, G. P. Yap, D. A. Lutterman, J. Rosenthal, *ACS Catal.* **2013**, *3*, 1685–1692.
- [9] a) G. Fiorani, W. Guo, A. W. Kleij, *Green Chem.* **2015**, *17*, 1375–1389; b) Y. Zhang, J. Y. G. Chan, *Energy Environ. Sci.* **2010**, *3*, 408–417; c) Y. Oh, X. Hu, *Chem. Soc. Rev.* **2013**, *42*, 2253–2261; d) L. Yang, H. Wang, *ChemSusChem* **2014**, *7*, 962–998.
- [10] a) S. Wang, X. Wang, *Small* **2015**, *11*, 3097–3112; b) J. L. Wang, C. Wang, W. Lin, *ACS Catal.* **2012**, *2*, 2630–2640; c) T. Zhang, W. Lin, *Chem. Soc. Rev.* **2014**, *43*, 5982–5993; d) Y. Fu, D. Sun, Y. Chen, R. Huang, Z. Ding, X. Fu, Z. Li, *Angew. Chem. Int. Ed.* **2012**, *51*, 3364–3367; *Angew. Chem.* **2012**, *124*, 3420–3423; e) J. Liu, P. K. Thallapally, B. P. McGrail, D. R. Brown, J. Liu, *Chem. Soc. Rev.* **2012**, *41*, 2308–2322; f) J. R. Li, R. J. Kuppler, H. C. Zhou, *Chem. Soc. Rev.* **2009**, *38*, 1477–1504.
- [11] a) S. Zhang, J. Sun, X. Zhang, J. Xin, Q. Miao, J. Wang, *Chem. Soc. Rev.* **2014**, *43*, 7838–7869; b) D. Grills, E. Fujita, *J. Phys. Chem. Lett.* **2010**, *1*, 2709–2718; c) Z. Z. Yang, Y. N. Zhao, L. N. He, *RSC Adv.* **2011**, *1*, 545–567.
- [12] T. Welton, *Chem. Rev.* **1999**, *99*, 2071.
- [13] a) J. Dupont, G. S. Fonseca, A. P. Umpierre, P. F. Fichtner, S. R. Teixeira, *J. Am. Chem. Soc.* **2002**, *124*, 4228–4229; b) S. N. Riduan, Y. Zhang, *Chem. Soc. Rev.* **2013**, *42*, 9055; c) P. Migowski, J. Dupont, *Chem. Eur. J.* **2007**, *13*, 32–39; d) J. Dupont, P. A. Suarez, *Phys. Chem. Chem. Phys.* **2006**, *8*, 2441–2452; e) J. E. Bara, T. K. Carlisle, C. J. Gabriel, D. Camper, A. Finotello, D. L. Gin, R. D. Noble, *Ind. Eng. Chem. Res.* **2009**, *48*, 2739–2751.
- [14] H. D. Velazquez, F. Verpoort, *Chem. Soc. Rev.* **2012**, *41*, 7032.
- [15] a) L. Mercs, M. Albrecht, *Chem. Soc. Rev.* **2010**, *39*, 1903–1912; b) Y. Zhang, E. Y. X. Chen, *Angew. Chem. Int. Ed.* **2012**, *51*, 2465–2469; *Angew. Chem.* **2012**, *124*, 2515–2519; c) A. T. Biju, N. Kuhl, F. Glorius, *Acc. Chem. Res.* **2011**, *44*, 1182–1195.
- [16] a) H. Hayashi, A. P. Cote, H. Furukawa, M. O’Keeffe, O. M. Yaghi, *Nat. Mater.* **2007**, *6*, 501–506; b) J. P. Zhang, Y. B. Zhang, J. B. Lin, X. M. Chen, *Chem. Rev.* **2012**, *112*, 1001–1033; c) M. Eddaoudi, D. F. Sava, J. F. Eubank, K. Adil, V. Guillerme, *Chem. Soc. Rev.* **2015**, *44*, 228–249.
- [17] a) R. Banerjee, A. Phan, B. Wang, C. Knobler, H. Furukawa, M. O’Keeffe, O. M. Yaghi, *Science* **2008**, *319*, 939–943; b) B. Wang, A. P. Côté, H. Furukawa, M. O’Keeffe, O. M. Yaghi, *Nature* **2008**, *453*, 207–211; c) K. S. Park, Z. Ni, A. P. Côté, J. Y. Choi, R. Huang, F. J. Uribe-Romo, H. K. Chae, M. O’Keeffe, O. M. Yaghi, *Proc. Natl. Acad. Sci. USA* **2006**, *103*, 10186–10191.
- [18] S. Wang, W. Yao, J. Lin, Z. Ding, X. Wang, *Angew. Chem. Int. Ed.* **2014**, *53*, 1034–1038; *Angew. Chem.* **2014**, *126*, 1052–1056.
- [19] a) J. E. Bara, D. E. Camper, D. L. Gin, R. D. Noble, *Acc. Chem. Res.* **2010**, *43*, 152–159; b) J. F. Brennecke, B. E. Gurkan, *J. Phys. Chem. Lett.* **2010**, *1*, 3459–3464; c) M. Ramdin, T. W. de Loos, T. J. H. Vlught, *Ind. Eng. Chem. Res.* **2012**, *51*, 8149–8177.
- [20] L. A. Blanchard, D. Hancu, E. J. Beckman, J. F. Brennecke, *Nature* **1999**, *399*, 28–29.
- [21] a) J. L. Anthony, J. L. Anderson, E. J. Maginn, J. F. Brennecke, *J. Phys. Chem. B* **2005**, *109*, 6366; b) S. N. Aki, B. R. Mellein, E. M. Saurer, J. F. Brennecke, *J. Phys. Chem. B* **2004**, *108*, 20355–20365; c) L. A. Blanchard, Z. Gu, J. F. Brennecke, *J. Phys. Chem. B* **2001**, *105*, 2437–2444.
- [22] a) C. Cadena, J. L. Anthony, J. K. Shah, T. I. Morrow, J. F. Brennecke, E. J. Maginn, *J. Am. Chem. Soc.* **2004**, *126*, 5300–5308; b) X. Huang, C. J. Margulis, Y. Li, B. J. Berne, *J. Am. Chem. Soc.* **2005**, *127*, 17842–17851.
- [23] E. D. Bates, R. D. Mayton, I. Ntai, J. H. Davis, *J. Am. Chem. Soc.* **2002**, *124*, 926–927.
- [24] G. Gurau, H. Rodríguez, S. P. Kelley, P. Janiczek, R. S. Kalb, R. D. Rogers, *Angew. Chem. Int. Ed.* **2011**, *50*, 12024–12026; *Angew. Chem.* **2011**, *123*, 12230–12232.
- [25] C. Wang, H. Luo, X. Luo, H. Li, S. Dai, *Green Chem.* **2010**, *12*, 2019–2023.
- [26] C. Wang, H. Luo, D. Jiang, H. Li, S. Dai, *Angew. Chem. Int. Ed.* **2010**, *49*, 5978–5981; *Angew. Chem.* **2010**, *122*, 6114–6117.
- [27] C. Wang, X. Luo, H. Luo, D. Jiang, H. Li, S. Dai, *Angew. Chem. Int. Ed.* **2011**, *50*, 4918–4922; *Angew. Chem.* **2011**, *123*, 5020–5024.
- [28] a) Y. Xie, Z. Zhang, T. Jiang, J. He, B. Han, T. Wu, K. Ding, *Angew. Chem. Int. Ed.* **2007**, *46*, 7255–7258; *Angew. Chem.* **2007**, *119*, 7393–7396; b) Y. Zhao, B. Yu, Z. Yang, H. Zhang, L. Hao, X. Gao, Z. Liu, *Angew. Chem. Int. Ed.* **2014**, *53*, 5922–5925; *Angew. Chem.* **2014**, *126*, 6032–6035.
- [29] F. Shi, Y. Deng, T. SiMa, J. Peng, Y. Gu, B. Qiao, *Angew. Chem. Int. Ed.* **2003**, *42*, 3257; *Angew. Chem.* **2003**, *115*, 3379.
- [30] Z. Zhang, Y. Xie, W. Li, S. Hu, J. Song, T. Jiang, B. Han, *Angew. Chem. Int. Ed.* **2008**, *47*, 1127; *Angew. Chem.* **2008**, *120*, 1143.
- [31] B. A. Rosen, A. Salehi-Khojin, M. R. Thorson, W. Zhu, D. T. Whipple, P. J. A. Kenis, R. I. Masel, *Science* **2011**, *334*, 643.
- [32] a) K. Chandrasekaran, J. O. M. Bockris, *Surf. Sci.* **1987**, *185*, 495–514; b) J. O. M. Bockris, J. C. Wass, *J. Electrochem. Soc.* **1989**, *136*, 2521–2528.
- [33] a) P. F. Yan, M. Yang, X. M. Liu, Q. S. Liu, Z. C. Tan, U. Welz-Biermann, *J. Chem. Eng. Data* **2010**, *55*, 2444–2450; b) D. Seth, A. Chakraborty, P. Setua, N. Sarkar, *J. Phys. Chem. B* **2007**, *111*,

- 4781–4787; c) O. A. El Seoud, A. Koschella, L. C. Fidale, S. Dorn, T. Heinze, *Biomacromolecules* **2007**, *8*, 2629–2647.
- [34] J. Lin, Z. Ding, Y. Hou, X. Wang, *Sci. Rep.* **2013**, *3*, 1056.
- [35] a) H. Zhou, Y. M. Wang, W. Z. Zhang, J. P. Qu, X. B. Lu, *Green Chem.* **2011**, *13*, 644–650; b) J. D. Holbrey, W. M. Reichert, I. Tkatchenko, E. Bouajila, O. Walter, I. Tommasi, R. D. Rogers, *Chem. Commun.* **2003**, 28–29; c) A. M. Voutchkova, L. N. Appelhans, A. R. Chianese, R. H. Crabtree, *J. Am. Chem. Soc.* **2005**, *127*, 17624–17625; d) H. Zhou, W. Z. Zhang, C. H. Liu, J. P. Qu, X. B. Lu, *J. Org. Chem.* **2008**, *73*, 8039–8044.
- [36] H. A. Duong, T. N. Tekavec, A. M. Arif, J. Louie, *Chem. Commun.* **2004**, 112–113.
- [37] a) E. Theuergarten, T. Bannenberg, M. D. Walter, D. Holschumacher, M. Freytag, C. G. Daniliuc, P. G. Jones, M. Tamm, *Dalton Trans.* **2014**, *43*, 1651–1662; b) M. J. Ajitha, C. H. Suresh, *Tetrahedron Lett.* **2011**, *52*, 5403–5406; c) P. L. Arnold, I. A. Marr, S. Zlatogorsky, R. Bellabarba, R. P. Tooze, *Dalton Trans.* **2014**, *43*, 34–37.
- [38] M. J. Ajitha, C. H. Suresh, *J. Org. Chem.* **2012**, *77*, 1087–1094.
- [39] R. Lo, B. Ganguly, *New J. Chem.* **2012**, *36*, 2549–2554.
- [40] M. Vogt, J. E. Bennett, Y. Huang, C. Wu, W. F. Schneider, J. F. Brennecke, B. L. Ashfeld, *Chem. Eur. J.* **2013**, *19*, 11134–11138.
- [41] H. Zhou, W. Z. Zhang, Y. M. Wang, J. P. Qu, X. B. Lu, *Macromolecules* **2009**, *42*, 5419–5421.
- [42] L. Gu, Y. Zhang, *J. Am. Chem. Soc.* **2010**, *132*, 914–915.
- [43] a) I. I. F. Boogaerts, G. C. Fortman, M. R. L. Furst, C. S. J. Cazin, S. P. Nolan, *Angew. Chem. Int. Ed.* **2010**, *49*, 8674–8677; *Angew. Chem.* **2010**, *122*, 8856–8859; b) H. Zhao, Z. Lin, T. B. Marder, *J. Am. Chem. Soc.* **2006**, *128*, 15637–15643; c) T. Ohishi, L. Zhang, M. Nishiura, Z. Hou, *Angew. Chem. Int. Ed.* **2011**, *50*, 8114–8117; *Angew. Chem.* **2011**, *123*, 8264–8267.
- [44] D. S. Laitar, P. Müller, J. P. Sadighi, *J. Am. Chem. Soc.* **2005**, *127*, 17196–17197.
- [45] T. Ohishi, M. Nishiura, Z. Hou, *Angew. Chem. Int. Ed.* **2008**, *47*, 5792–5795; *Angew. Chem.* **2008**, *120*, 5876–5879.
- [46] D. Yu, Y. Zhang, *Proc. Natl. Acad. Sci. USA* **2010**, *107*, 20184–20189.
- [47] a) A. Rit, T. P. Spaniol, L. Maron, J. Okuda, *Angew. Chem. Int. Ed.* **2013**, *52*, 4664–4667; *Angew. Chem.* **2013**, *125*, 4762–4765; b) I. I. F. Boogaerts, S. P. Nolan, *J. Am. Chem. Soc.* **2010**, *132*, 8858–8859; c) M. Yamashita, K. Goto, T. Kawashima, *J. Am. Chem. Soc.* **2005**, *127*, 7294–7295; d) P. W. Ariyananda, G. P. Yap, J. Rosenthal, *Dalton Trans.* **2012**, *41*, 7977–7983; e) C. H. Lee, D. S. Laitar, P. Mueller, J. P. Sadighi, *J. Am. Chem. Soc.* **2007**, *129*, 13902–13903.
- [48] S. N. Riduan, Y. Zhang, J. Y. Ying, *Angew. Chem. Int. Ed.* **2009**, *48*, 3322–3325; *Angew. Chem.* **2009**, *121*, 3372–3375.
- [49] E. L. Kolychev, T. Bannenberg, M. Freytag, C. G. Daniliuc, P. G. Jones, M. Tamm, *Chem. Eur. J.* **2012**, *18*, 16938–16946.
- [50] F. Huang, G. Lu, L. Zhao, H. Li, Z. X. Wang, *J. Am. Chem. Soc.* **2010**, *132*, 12388–12396.
- [51] S. N. Riduan, J. Y. Ying, Y. Zhang, *ChemCatChem* **2013**, *5*, 1490–1496.
- [52] Y. Kayaki, M. Yamamoto, T. Ikariya, *Angew. Chem. Int. Ed.* **2009**, *48*, 4194–4197; *Angew. Chem.* **2009**, *121*, 4258–4261.
- [53] V. S. Thoi, N. Kornienko, C. G. Margarit, P. Yang, C. J. Chang, *J. Am. Chem. Soc.* **2013**, *135*, 14413–14424.
- [54] D. M. Denning, M. D. Thum, D. E. Falvey, *Org. Lett.* **2015**, *17*, 4152–4155.
- [55] a) R. Banerjee, H. Furukawa, D. Britt, C. Knobler, M. O’Keeffe, O. M. Yaghi, *J. Am. Chem. Soc.* **2009**, *131*, 3875–3877; b) A. Phan, C. J. Doonan, F. J. Uribe-Romo, C. B. Knobler, M. O’Keeffe, O. M. Yaghi, *Acc. Chem. Res.* **2010**, *43*, 58–67.
- [56] W. Morris, B. Leung, H. Furukawa, O. K. Yaghi, N. He, H. Hayashi, Y. Houndonougbo, M. Asta, B. B. Laird, O. M. Yaghi, *J. Am. Chem. Soc.* **2010**, *132*, 11006–11008.
- [57] C. Zhang, Y. Xiao, D. Liu, Q. Yang, C. Zhong, *Chem. Commun.* **2013**, *49*, 600–602.
- [58] a) S. R. Venna, M. A. Carreon, *J. Am. Chem. Soc.* **2010**, *132*, 76–78; b) O. Tzialla, C. Veziri, X. Papatryfon, K. Beltsios, A. Labropoulos, B. Iliev, G. Adamova, T. Schubert, M. Kroon, M. Francisco, *J. Phys. Chem. C* **2013**, *117*, 18434–18440; c) B. Seoane, J. Coronas, I. Gascon, M. E. Benavides, O. Karvan, J. Caro, F. Kapteijn, J. Gascon, *Chem. Soc. Rev.* **2015**, *44*, 2421–2454; d) J. Gascon, F. Kapteijn, *Angew. Chem. Int. Ed.* **2010**, *49*, 1530–1532; *Angew. Chem.* **2010**, *122*, 1572–1574; e) Y. S. Li, H. Bux, A. Feldhoff, G. L. Li, W. S. Yang, J. Caro, *Adv. Mater.* **2010**, *22*, 3322–3326; f) T. H. Bae, J. S. Lee, W. Qiu, W. J. Koros, C. W. Jones, S. Nair, *Angew. Chem. Int. Ed.* **2010**, *49*, 9863–9866; *Angew. Chem.* **2010**, *122*, 10059–10062.
- [59] C. M. Miralda, E. E. Macias, M. Zhu, P. Ratnasamy, M. A. Carreon, *ACS Catal.* **2012**, *2*, 180–183.
- [60] T. Jose, Y. Hwang, D. W. Kim, M. I. Kim, D. W. Park, *Catal. Today* **2015**, *245*, 61–67.
- [61] S. Wang, Y. Hou, S. Lin, X. Wang, *Nanoscale* **2014**, *6*, 9930–9934.
- [62] S. Wang, J. Lin, X. Wang, *Phys. Chem. Chem. Phys.* **2014**, *16*, 14656–14660.
- [63] S. Wang, X. Wang, *Appl. Catal. B* **2015**, *162*, 494–500.
- [64] a) K. Maeda, R. Kuriki, M. Zhang, X. Wang, O. Ishitani, *J. Mater. Chem. A* **2014**, *2*, 15146–15151; b) R. Kuriki, K. Sekizawa, O. Ishitani, K. Maeda, *Angew. Chem. Int. Ed.* **2015**, *54*, 2406–2409; *Angew. Chem.* **2015**, *127*, 2436–2439; c) C. Huang, C. Chen, M. Zhang, L. Lin, X. Ye, S. Lin, M. Antonietti, X. Wang, *Nat. Commun.* **2015**, *6*, 7698; d) Y. Zheng, L. Lin, X. Ye, F. Guo, X. Wang, *Angew. Chem. Int. Ed.* **2014**, *53*, 11926–11930; *Angew. Chem.* **2014**, *126*, 12120–12124; e) F. Goettmann, A. Thomas, M. Antonietti, *Angew. Chem. Int. Ed.* **2007**, *46*, 2717–2720; *Angew. Chem.* **2007**, *119*, 2773–2776; f) J. Qin, S. Wang, H. Ren, Y. Hou, X. Wang, *Appl. Catal. B* **2015**, *179*, 1–8; g) Y. Zheng, L. Lin, B. Wang, X. Wang, *Angew. Chem. Int. Ed.* **2015**, *54*, 12868–12884; *Angew. Chem.* **2015**, *127*, 13060–13077; h) J. Zhang, Y. Chen, X. Wang, *Energy Environ. Sci.* **2015**, *8*, 3092–3108.

Received: July 31, 2015

Revised: September 10, 2015

Published online: December 18, 2015